Journal of Microbiology (2021) Vol. 59, No. 11, pp. 988–1001
DOI 10.1007/s12275-021-1271-9
eISSN 1976-3794
pISSN 1225-8873

The comparison of microbial communities in thyroid tissues from thyroid carcinoma patients

Chen-Jian Liu[1†], Si-Qian Chen[1†], Si-Yao Zhang[1], Jia-Lun Wang[1], Xiao-Dan Tang[2,3], Kun-Xian Yang[4,5*], and Xiao-Ran Li[1*]

[1]*Faculty of Life Science and Technology, Kunming University of Science and Technology, Kunming 650500, Yunnan, P. R. China*
[2]*Gastroenterology Department, the First People's Hospital of Yunnan Province, Kunming 650032, Yunnan, P. R. China*
[3]*Gastroenterology Department, the Affiliated Hospital of Kunming University of Science and Technology, Kunming 650032, Yunnan, P. R. China*
[4]*Oncology Department, the First People's Hospital of Yunnan Province, Kunming 650032, Yunnan, P. R. China*
[5]*Oncology Department, The Affiliated Hospital of Kunming University of Science and Technology, Kunming 650032, Yunnan, P. R. China*

(Received May 20, 2021 / Revised Aug 17, 2021 / Accepted Aug 20, 2021)

Thyroid carcinoma is a common endocrine organ cancer associated with abnormal hormone secretion, leading to the disorder of metabolism. The intestinal microbiota is vital to maintain digestive and immunologic homeostasis. The relevant information of the microbial community in the gut and thyroid, including composition, structure, and relationship, is unclear in thyroid carcinoma patients. A total of 93 samples from 25 patients were included in this study. The results showed that microbial communities existed in thyroid tissue; gut and thyroid had high abundance of facultative anaerobes from the Proteobacteria phyla. The microbial metabolism from the thyroid and gut may be affected by the thyroid carcinoma cells. The cooccurrence network showed that the margins of different thyroid tissues were unique areas with more competition; the stabilization of microcommunities from tissue and stool may be maintained by several clusters of species that may execute different vital metabolism processes dominantly that are attributed to the microenvironment of cancer.

Keywords: thyroid carcinoma, thyroid microbiota, cooccurrence network, Tax4Fun2, gut microbiota

Introduction

Thyroid carcinoma is the most common malignant tumor of the endocrine system and accounts for approximately 1% of all newly diagnosed cancer cases (Hubbell, 2005). The most frequent type of thyroid malignancy is papillary carcinoma, which constitutes approximately 80% of all cases (Nikiforov, 2008). The incidence of well-differentiated thyroid carcinoma has been increasing dramatically over the last 20 years worldwide and is expected to be the fourth most common cancer by 2030 (Rahib *et al.*, 2014). Epidemiological analysis of cancer registries in Europe (Akslen *et al.*, 1993; McNally *et al.*, 2010; Olaleye *et al.*, 2011; Londero *et al.*, 2015), America (Zheng *et al.*, 1996; Liu *et al.*, 2001), the middle east (Lubina *et al.*, 2006), and Asia (Saika *et al.*, 2014; Xie *et al.*, 2014; Wang and Wang, 2015) have shown an increase in almost all types of thyroid tumor due to a clear birth cohort effect, whereas other studies have also identified a time-period effect, suggesting that both events occur simultaneously. Thus, identifying new risk factors for thyroid carcinoma and understanding temporal changes in both established and new risk factors represent an increasingly important public health priority.

In many cases, cancer is considered to be associated with human microorganisms, especially enteric microorganisms. The intestinal microbiota is essential for the host to ensure digestive and immunologic homeostasis. When microbiota homeostasis is impaired and dysbiosis occurs, the malfunction of the epithelial barrier leads to intestinal and systemic disorders, chiefly immunologic and metabolic (Virili and Centanni, 2015). The host microbiota is crucial not only for digestive equilibrium but also immunologic, hormonal, and metabolic homeostasis. It is not surprising that when microbiota homeostasis is impaired and dysbiosis occurs, the malfunction of the epithelial barrier may ensue, and local and general disorders may develop. A pathogenetic link with dysbiosis has been described for obesity, type II diabetes, and inflammatory bowel diseases as well as autoimmune disorders such as multiple sclerosis, type I diabetes, and rheumatic diseases (Tlaskalová-Hogenová *et al.*, 2011). In mice and humans, the intestine houses a large part of the immune system, and the gut possesses more immunoglobulin-secreting cells than any other lymphoid organ (Hrdina *et al.*, 2009; Faria *et al.*, 2013).

Autoimmune thyroid disease is the most frequent autoimmune disorder, and hypo- and hyperthyroidism, often of autoimmune origin, are associated with bacterial overgrowth (Lauritano *et al.*, 2007) and with a different microbiota composition, respectively (Zhou *et al.*, 2014). More evidence has indicated a strong correlation between gut microbiota and diseases outside the gut (liver tumor, cholelithiasis, osteoarthritis, etc.) (Jackson *et al.*, 2018; NIH/National Cancer Institute, 2018). Gut microbiota composition and the thyroid-related micronutrients iodine and selenium have a key role in maintaining thyroid homeostasis. Bacterial action may deeply affect the enzymatic activity, and thus, microbiota composition may be involved in a crucial path of thyroid ho-

†These authors contributed equally to this work.
*For correspondence. (X.R. Li) E-mail: starkeyran@163.com; Tel.: +86-871-65920759; Fax: +86-871-65920759 / (K.X. Yang) E-mail: khyy157@126.com; Tel.: +86-871-63639921; Fax: +86-871-63627731

meostasis (Hrdina *et al.*, 2009; NIH/National Cancer Institute, 2018). Moreover, gut, oral, and skin microbiomes have been illustrated in various research and the lung was recently confirmed to be colonized with microbiome (Wypych *et al.*, 2019). Whether there is any correlation between thyroid tumor and gut, the existence of microbiota species, their interaction, phylocoenogenesis situation and the effect on tumors in the thyroid remain mysteries. In this study, we hope to elucidate the microbial construction of the thyroid and intestine to determine whether thyroid microorganisms are delivered from the intestine and how thyroid tumors influence microbial communities.

Materials and Methods

Subject recruitment and clinical information

The protocol for the original treatment study was approved by the Medical ethics committee of Kunming University of Science and Technology (number: KMUST-MEC-081). All research methods were performed by the relevant guidelines and regulations. For the consent process, we contacted patients or their family members and explained the study in detail. After the informed consent process, all 25 families agreed to participate and signed written parent permission and assent forms. We maintained the confidentiality of participants' results by de-identifying all samples of the entire analysis. The participant's name and identifiers were removed and not used in all sections of the manuscript.

All the samples were collected at the Breast and Thyroid Surgery of The First People's Hospital of Yunnan Province, China in 2017. To reduce the impact on environment, samples were collected within one month, and the follow-up study was only open to adult with thyroid tumor who lives in Yunnan province. During this period, 25 thyroid patients (age 25–66) were recruited (Table 1). All of them were without pro or antibiotic treatment (approximately one month) and evidence of recent infections, nursing or pregnant women before sample collection. When they were hospitalized, fatty, spicy, smoked foods, smoke, and alcohol were forbidden. Tumor identification was based on organized testing as well as imagological examination. All tissue samples were taken during surgery for therapeutic reasons.

Sample collection

To avoid the potential confounding of environmental factors, tissue samples were removed from the thyroid in the operating room during surgery, divided into tumor, para-tumor and normal tissues, and packaged in aseptic bags as soon as possible. Stool samples were collected before the operation, with immediate placement in aseptic centrifuge tubes. Sampling equipment and containers were strictly sterile. Each time during sample collection, we opened another three containers with exposure to the environment as negative controls. All samples were stored at -20°C to inhibit bacterial growth until DNA extraction within one day. The informed consent was obtained from participants before sample collection in this study. Of the 93 samples available from thyroid patients (19 malignant and six benign patients), we extracted the 16S rRNA gene sequences of microbes from tumor issue, para-carcinoma issue, normal issue and stool.

DNA preparation, PCR amplification, and sequencing

A frozen aliquot (approximately 1 g) of both tissue and stool sample was frozen by liquid nitrogen four to five times, ground, and made into a uniformly fine powder for DNA extraction. To avoid contamination, each mortar used in the grinding process was cleaned and dried (5 h) at approximately 200°C. Total DNA was extracted as described (Schmidt *et al.*, 1991). In this extraction process, after purchase, all reagents were separated on a newly purchased (without microbial or molecular biology-related experiments) super-clean table as soon as possible. Each sample was treated with an independent reagent group. DNA yield was evaluated by the Nanodrop 2000 (Thermo Fisher). For each sample, the bacterial and archaeal 16S rRNA genes were amplified with the barcoded primer set 515F (Reysenbach *et al.*, 1992) and 909R (Brunk and Eis, 1998) including the Illumina MiSeq adapter sequences. All PCR amplifications were performed with *pfu* DNA Master-Mix (Tiangen) in a total volume of 50 μl containing 15 ng of DNA added as template (the annealing temperature was 51°C). In the process of each DNA extraction as well as PCR batching, two negative controls with the same reagents and consumables were handled using the same procedure. Amplicons were purified using the UltraClean PCR Clean-up kit (MO BIO), and an equivalent amount of PCR product was mixed for sequencing using the Illumina MiSeq™ system (Illumina). Negative controls could not be detected by Nanodrop 2000 (Thermo Fisher) after PCR amplification.

Sequence analysis and statistics

All sequences were demultiplexed using the barcodes of each

Table 1. General characteristics of the patients with thyroid cancer enrolled in this study, including tumor type, age, gender, numbers of sample, etc.

Characteristic	All	Malignant	Benign	*p*
Patient numbers	25	19	6	/
Tumor	26	19	7	/
Para-tumor	26	19	7	/
Normal tissue	24	17	7	/
Stool	17	12	5	/
Age (Mean ± SD)	45.3 ± 11.2	42.6 ± 9.9	54.0 ± 11.6	0.026138015 < 0.05
Male	10	8	2	/
Female	15	11	4	/
With other diseases	8	6	2	/

sample. Sequence processing was performed by combining features of Mothur v1.43.0 (Schloss *et al.*, 2009) according to the MiSeq SOP. The SSU rRNA database sequences and taxonomic information from SILVA (v132) (Pruesse *et al.*, 2007) were downloaded directly from the Mothur website. Chimera checking was performed after the sequences were aligned. Similar sequences were clustered into OTUs (Operational Taxonomical Units) with a minimum identity of 97%. OTU with only one sequence in one sample was excluded. In Conet analysis, we filtered OTUs that were less than 0.02% sequences in total for further analysis. The distance matrix and principal coordinate analysis (PCoA) were analyzed by Jclass method. The community types were defined based on Dirichlet multinomial mixtures, as described by Holmes *et*

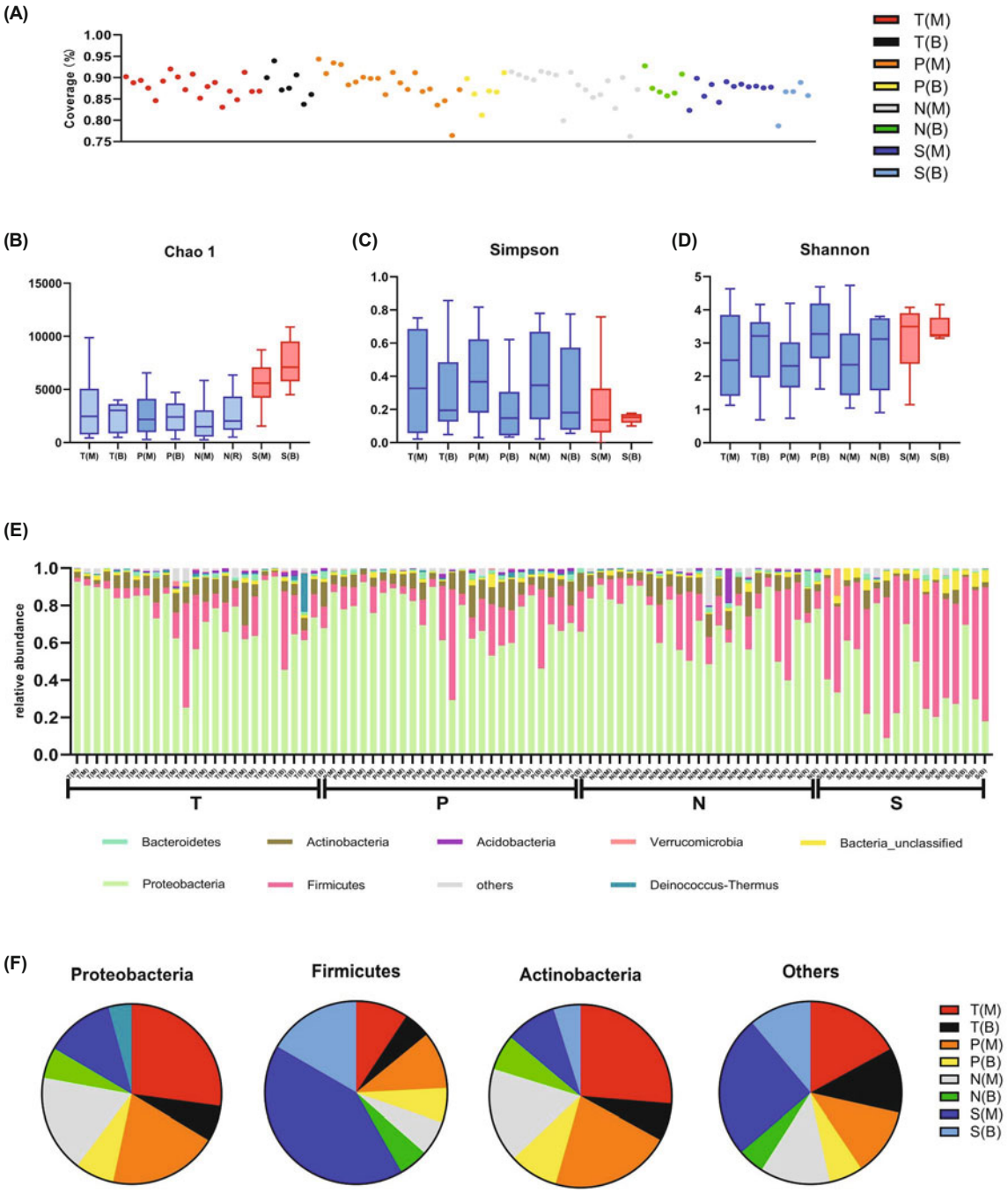

Fig. 1. Microbiota abundance and compositions in different groups. (A) Concentration of total DNA extracted from each sample. (B, C, and D) Alpha-diversity box-whisker plots of OTU number, taxon richness (Chao1 indices) and diversity (Shannon–Wiener and Simpson indices) in samples analyzed by 16S rRNA gene sequencing. (E) Relative abundances of bacterial taxa identified at the phylum level for each sample. (F) Diversity of the most abundant bacterial taxa identified at the phylum level in different groups. Taxonomic assignment of 16S rRNA sequences was carried out using OTU with the SILVA SSU database v132 with a cutoff of 97% homology. T, tumor; P, para-tumor; N, normal tissue; S, stool; M, malignant; B, benign.

al. (2012); this approach was used because it allows for clustering from unevenly sampled populations. Statistical analysis was completed using EXCEL 2016 and GraphPad Prism 8.

Phylogenetic trees were constructed via MEGA-X (Kumar *et al*., 2018) with the neighbor joining method. The NTI were conducted using the 'picante' R package (Kembel *et al*., 2010).

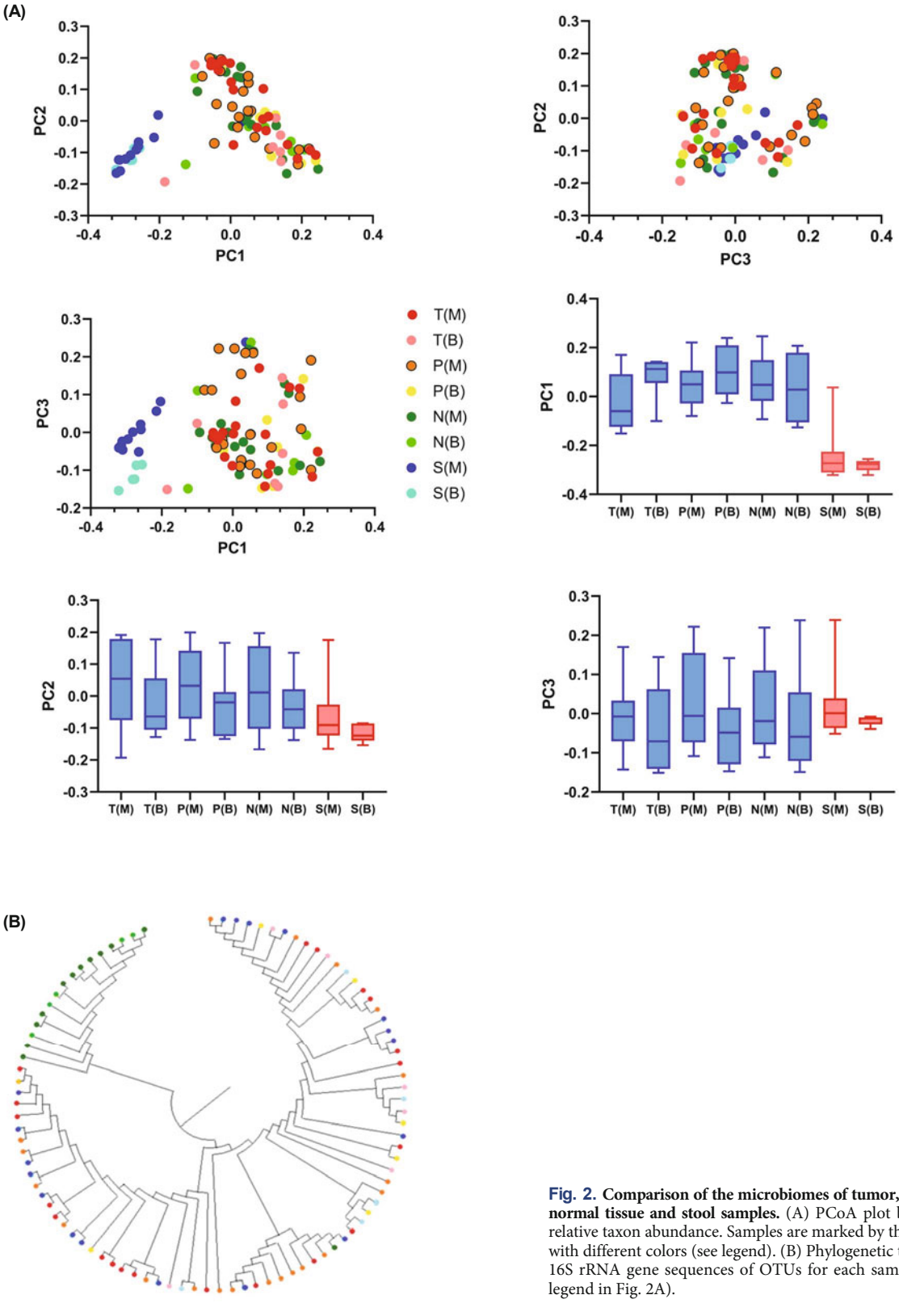

Fig. 2. Comparison of the microbiomes of tumor, para-tumor, normal tissue and stool samples. (A) PCoA plot based on the relative taxon abundance. Samples are marked by the group type with different colors (see legend). (B) Phylogenetic tree based on 16S rRNA gene sequences of OTUs for each sample type (see legend in Fig. 2A).

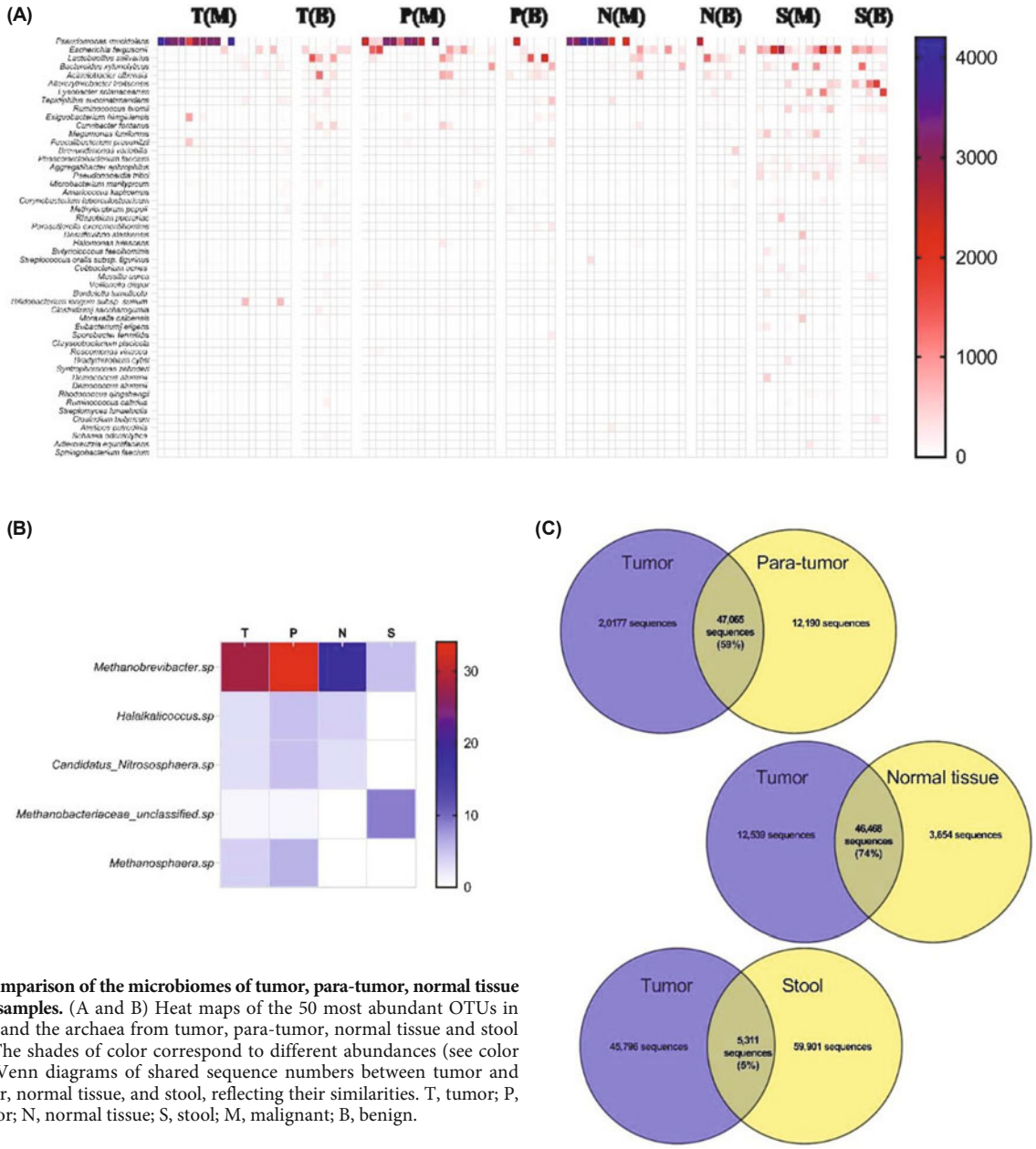

Fig. 3. Comparison of the microbiomes of tumor, para-tumor, normal tissue and stool samples. (A and B) Heat maps of the 50 most abundant OTUs in all groups and the archaea from tumor, para-tumor, normal tissue and stool samples. The shades of color correspond to different abundances (see color bar). (C) Venn diagrams of shared sequence numbers between tumor and para-tumor, normal tissue, and stool, reflecting their similarities. T, tumor; P, para- tumor; N, normal tissue; S, stool; M, malignant; B, benign.

The network was constructed using Cytoscape 3.7.2 (www://www.cytoscape.org/). The cooccurrence network was constructed with 'conet' (Faust *et al.*, 2012) in Cytoscape 3.7.2 based on the settings of (Faust *et al.*, 2012), and the subnetworks were extracted by 'MCODE' (Bader and Hogue, 2003) Cytoscape software. We defined the nodes as network hubs (z-score > 2.5; c-score > 0.6), module hubs (z-score > 2.5; c-score < 0.6), connectors (z-score < 2.5; c-score > 0.6) and peripherals (z-score < 2.5; c-score < 0.6), referring to their roles in network structure (Poudel *et al.*, 2016). This analysis was calculated by 'GIANT' (Cumbo *et al.*, 2014) Cytoscape software with the Spectral cluster method. Functional predictions were performed using Tax4Fun2 (Wemheuer *et al.*, 2020).

Nucleotide sequence availability

The PCR product sequencing data in this study were deposited in the Short Read Archive of NCBI under the accession number PRJNA637955.

Results

The abundance and composition of microbiota in different samples

The samples represented more than 220,000 high-quality reads in total (Fig. 1A). The average Good's coverage of the samples was 87.8%. The different α-diversity indices (OTU numbers and Chao1, Shannon and Simpson indices, shown

in Fig. 1B, C, and D) were different among all types of samples. In general, all fecal diversities were higher than those of tissues. Tissue samples from benign patients had a higher diversity, and the total number of microorganisms decreased with the increasing distance from the cancerous tissue. The OTU table contains 2,703 OTUs distributed over 24 bacterial phyla (Fig. 1E and F), with *Proteobacteria* as the most abundant phylum. Except in stool, we found that this phylum was prominent in the other three types of tissue samples, especially in malignant tumor patients, while *Firmicutes* was dominant in stool.

OTU-based analysis from eight groups

Based on OTU data, a PCoA and phylogenetic tree were constructed (Fig. 2A and B). PC1 showed that the stool samples (malignant and benign) were concentrated, while the other three types were widely separated and fell into clusters. At the same time, the phylogenetic trees revealed that the stool samples were almost clustered together. The top 50 OTUs abundant in samples showed that the high-abundant OTUs were concentrated in a few of the species in tissue samples, but stool had more species in this aspect (Fig. 3A). A total of 19 samples contained 32 OTUs belonging to archaea (Fig. 3B). The most abundant OTU was affiliated with *Methanobrevibacter* sp., which was detected in all sample types. These data illustrated that the composition of OTUs in tissue and stool were completely different.

Relationship between thyroid carcinoma and the gut microbial community

The bacterial sequences shared between tissues and stool are shown by Venn diagram in (Fig. 3C). Approximately half of sequences from tumors were shared among para-tumor and normal tissue, while only 5% of microbe sequences were

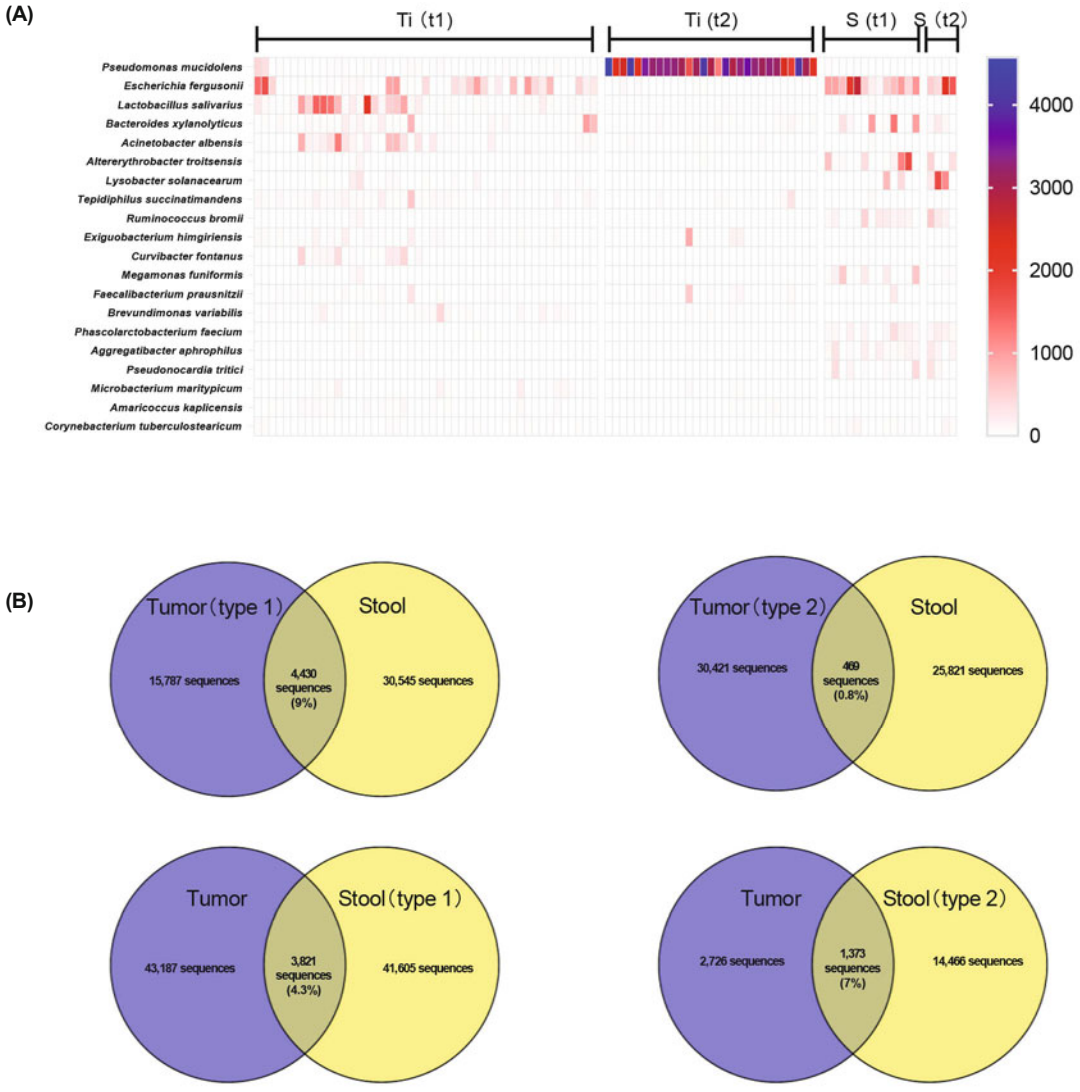

Fig. 4. The relationship of microbial composition in different community types. (A) Heat maps of the 20 most abundant OTUs in four communities found in all samples. Ti, thyroid tissue; S, stool; t1, type 1; t2, type 2. The shades of color correspond to different abundances (see color bar). (B) Venn diagrams of shared sequence numbers of different community types with individual corresponding microbial communities from thyroid tissue or stool.

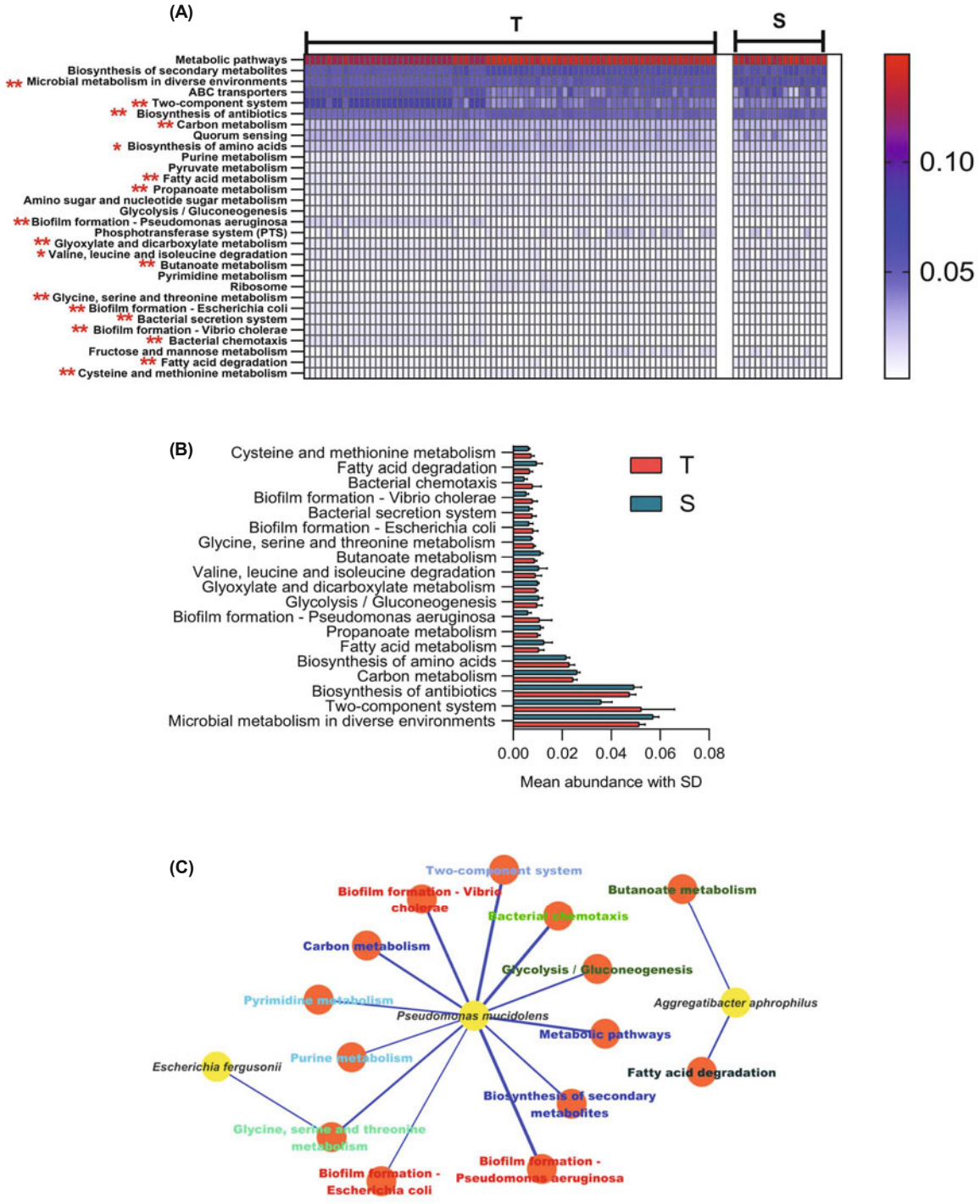

Fig. 5. Functional profiling of the bacterial communities by Tax4Fun2, cooccurrence network of the whole scale of thyroid microbial community and the phylocoenogenesis of tumor, para-tumor, normal tissue and stool samples. (A) Heat maps of the relative abundance of the top 30 pathways from thyroid tissues and stools. The shades of color correspond to different abundances (see color bar). Significant difference: *$p < 0.05$, T-test (two-tailed test); **$p < 0.01$, T-test (two-tailed test). (B) The relative abundance of significantly different pathways from thyroid tissues and stools (Mean ± SD). (C) Network of OTUs correlated with several processes among the top 30 pathways ($|r| > 0.6$, $p < 0.0001$, Pearson test).

shared between tumor and stool. The tissue samples and stool could be divided into two communities (Fig. 4A and B), both of them with a little overlap between two microbial communities from each patient. The community types were irrelevant to the age, sex, tumor character, or concomitant diseases. In summary, the microbiomes from thyroid had a few relevant correlations with stool.

The microenvironment of the thyroid organ is different from that of the gut. We performed a functional prediction of the bacterial communities using Tax4Fun2. A total of 350 path-

ways were concentrated, most of which were associated with metabolism. The most abundant pathways were evaluated by heat maps, and they could be mostly separated into bacterial interactions and cell metabolisms (Fig. 5A and B). All of them were involved in pyruvate, fatty acid metabolism and glycolysis or gluconeogenesis. Eighteen of the top 30 pathways were significantly different between thyroid and gut. We used a stochastic forest model to predict the major different OTUs

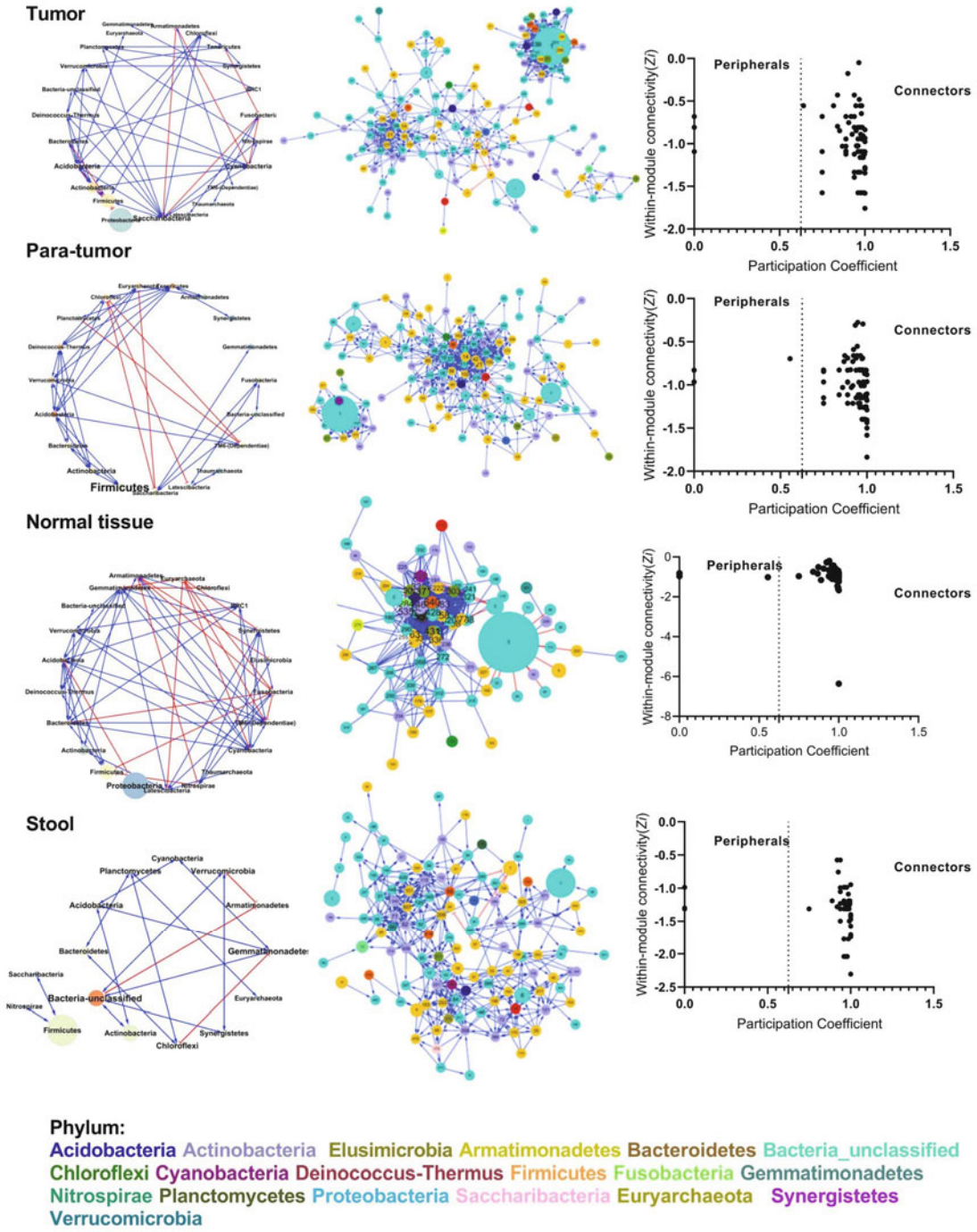

Fig. 6. Cooccurrence network of tumor, para-tumor, normal tissue and stool samples. (A) Cooccurrence network of four types of sample at the phylum (left) or OTU (middle) level. Sequences with more abundance are shown in a larger node. Nodes with a more direct neighborhood are shown with a larger label size. Red edge, negative relevance; Blue edge, positive relevance. In the phylum network, nodes with larger degree are filled in a brighter color; labels are shown for the different phylum. In the OTU network, species from different phyla are represented by different colors (corresponding to the phylum names in the graph); labels represent the OTU numbers. Topological properties of within-module connectivity and participation coefficient (right) based the OTU network are shown in the right of this Figure.

between these environments, and after filtering the data, three of the major microbes were found (*Brevundimonas variabilis*, *Phascolarctobacterium faecium*, and *Aggregatibacter aphrophilus*). *Aggregatibacter aphrophilus* was found to be closely relevant to fatty acid degradation and butanoate metabolism ($|r| > 0.6$, $p < 0.0001$, Pearson test), of which the abundances were different between thyroid and gut ($p < 0.01$; T-test [two-tailed test]). By the correlation test, we found that two of the most abundant OTUs, *Pseudomonas mucidolens* and *Escherichia fergusonii,* were associated with several processes ($|r| > 0.6$, $p < 0.0001$, Pearson test) (Fig. 5C).

Structures of the microbial community

A cooccurrence network was built for each sample type (tumor, para-tumor, normal issue and stool) with the relative abundances of phylum and OTUs (more than 99.9% with a 0.03 cutoff) as nodes and correlations between relative abundances (Fig. 6A). At the phylum level, most OTUs were from the phyla of Proteobacteria, Firmicutes and Actinobacteria. There were a greater number of negatively correlated edges in normal tissue (26%), para-tumor (13%), and stool (17%) compared with tumor (8%). In the tissue samples, as the distance

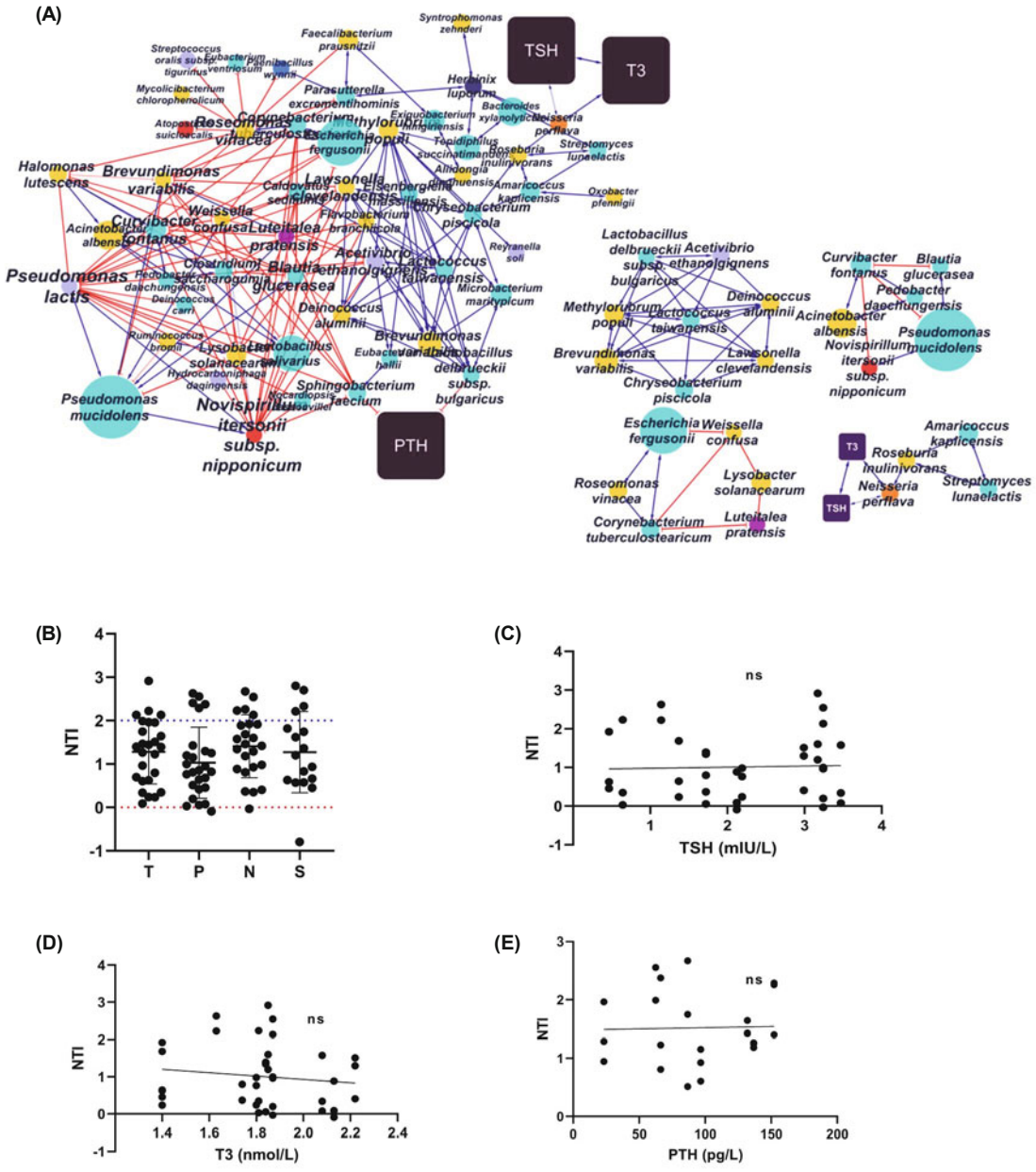

Fig. 7. (A) Cooccurrence network of the thyroid (including tumor, para-tumor and normal tissue from thyroid gland). Setting of the network referenced in Fig. 5A. c1-c4 are the subnetwork extracted from the whole of the thyroid. (B) Phylocoenogenesis situation in four types of samples; a score higher than zero means phylogenetic clustering, while a score less than zero means phylogenetic over-dispersion. Higher or less than ± 2 means significantly far from zero. (C, D, and E) The relationship of phylocoenogenesis between NTI and different hormones (T3, tri-iodothyronine; TSH, thyrotropin; PTH, parathyroid hormone; ns, not significant [$|r| < 0.6$, Pearson test]).

from the tumor increased, the percentage of negatively correlated edges increased. Most of the OTUs belonged to the phyla of Firmicutes, Actinobacteria and Proteobacteria. Network hubs are OTUs that are highly connected in general as well as within a module, and module hubs are interpreted as OTUs that are highly connected only within a module. Connectors are OTUs that are linked with modules, while peripherals have few links to other species (Poudel *et al.*, 2016). We did not observe any hubs in these networks, but there was a large proportion of connector nodes. Modules were not connected based on central nodes. To explore the phylocoenogenesis, we used null within-community models (nearest-taxon index [NTI]). NTI quantifies the standard deviations of the observed MNTD compared with random MNTD from the mean of the null distribution (999 randomizations). An NTI for a single community higher than zero indicates phylogenetic clustering, when less than zero indicates phylogenetic overdispersion (Fine and Kembel, 2011; Stegen *et al.*, 2012, 2013; Wang *et al.*, 2013). We found that nearly all of the samples were phylogenetically clustered, indicating that the community seems to be in the primary stage of community succession (Fig. 7B).

Based on the total number of tissue samples, we reconstructed a cooccurrence network that was associated with hormones (Fig. 7A). At this large scale, there were more negative edges between OTUs. Several microbes were negatively related with PTH, while *Neisseria perflava* was positively related with TSH and T3. We extracted four subsets from the network and found several microbes that were closely related to TSH and T3. NTI scores showed no significant relevance, with positive correlation with PTH and TSH, but negative with T3 (Fig. 7C, D, and E).

Discussion

Our study provided a complete illustration of the thyroid and gut microbial communities. We revealed the diversity of the microbial community and the microbial interactions in thyroid tissue and gut from thyroid carcinoma patients. Several microbial species that may be associated with cancer development were identified. These findings gave us a holistic understanding of microbial community in thyroid patients and provided a direction for further research of the linkage between microbes and cancer.

For a long time, except in the gut, the existence of microbes in humans in vivo has remained a mystery. A recent study found that in all types of tumor tissue, from cerebral cancer to osteosarcoma and breast cancer, bacterial communities exist (Nejman *et al.*, 2020). Our work provides a supplement of this study and confirmed that there was a microbial community in thyroid. Thus, the microbes detected in thyroid lead to a new speculation about the pathogenesis of thyroid carcinoma.

Previously, several studies revealed that diseases were correlated with enteric microorganisms and that gut bacteria may affect other organs through immune cells or secretases (Hu *et al.*, 2016; Vuong and Hsiao, 2017; Jia, 2019). A mass of sequences belonging to Proteobacteria was detected in thyroid and gut. The phylum of Proteobacteria, which are facultative anaerobes, at the individual level, are not dominant in healthy intestine, where there are extremely low levels of oxygen, and over 90% of gut microbiota are characterized as strict anaerobes (Chaudhary *et al.*, 2018). The high abundance of Proteobacteria may indicate the change of oxygen homeostasis or concentration in thyroid and intestinal tract. Moreover, a balanced gut microbiota with high stability will have symbiotic interactions with the immune system of the host, which is capable of suppressing the uncontrolled expansion of Proteobacteria. A bloom of Proteobacteria in the gut can reflect an unstable structure of the gut microbial community, a situation that can be observed in disease states (Shin *et al.*, 2015). In addition, with only a very partial overlap of sequences between thyroid and gut, even among the patients within the same community type of microbiome, we cannot suggest that there is a linkage between gut and thyroid microbes. However, the increasing number of Proteobacteria may be affected by thyroid carcinoma cells, giving rise to a unique community.

Many studies have shown that the microbiota can be an indicator to assess disease development and therapy outcomes. In colorectal cancer, *E. coli* and *Fusobacterium nucleatum* have been confirmed to be strongly related to tumor development (Gagnière *et al.*, 2017; Yu *et al.*, 2017). A considerable quantity of *Pseudomonas mucidolens* from three types of tissue samples was detected. *Pseudomonas mucidolens* is linked with food spoilage (Dzieciol *et al.*, 2016), as well as nonspecific polysaccharide-producing rhizosphere bacteria in an agricultural study (Ueno and Shetty, 1997), but it's status in thyroid carcinogenesis haven't been reported. In *Pseudomonas* genus, several members have been reported to be associated with infections such as bacteremia and lower respiratory tract infections in clinical research (Wu *et al.*, 2011; Scales *et al.*, 2014; Parkins *et al.*, 2018). Moreover, *Pseudomonas aeruginosa*, an opportunistic pathogen that causes various infections was considered to escalate its virulence and promotes systemic inflammation during host stress; human isolated *P. aeruginosa* promotes intestinal pathology and cancer-related epithelial phenotypes in genetically predisposed model hosts (Markou and Apidianakis, 2014). Nevertheless, recently an exotoxin (pseudomonas exotoxin A) with anti-tumor function, produced by several species in *Pseudomonas* has been reported. Besides, extracted exopolysaccharides (EPSs) secreted by *Pseudomonas* were considered with anti-tumor activities (Leshem and Pastan, 2019; Tahmourespour *et al.*, 2020). Thus, the characteristic of *Pseudomonas mucidolens* on diseases remains unclarified and requires further study. Since in the unhealthy condition of thyroid, we hypothesis that *Pseudomonas mucidolens* is a pathogen in carcinogenesis. In addition, with Tax4Fun2 analysis, we found that it was significantly associated with almost half of the processes among the top 30 pathways, including biofilm formation of two pathogens. From this result, like "driver-passenger" model in colorectal cancer, we thought that *Pseudomonas mucidolens* may promote cancerous process as driver bacteria, formed tumor microenvironment which is suitable for pathogens' colonization, leading to poor outcome (Avril and Depaolo, 2021).

The thyroid gland is a vital endocrine organ producing thyroxin. Thyroxin, including thyroxine (T4) and tri-iodothy-

ronine (T_3), are released by the stimulation of thyrotropin (TSH). TSH is secreted by the parathyroid gland, which is closely associated with the thyroid grand. This endocrine gland also produces parathyroid hormone (PTH), balancing the blood calcium levels. Approximately 10% of T4 undergoes monodeiodination to T3 before it is secreted and the released iodine is recycled. Later, 80% of the T4 undergoes peripheral conversion to the more active T3 in the liver and kidney (T3 is ten times more active than T4) or to reverse T3 (rT3), which has little or no biological activity (Nussey and Whitehead, 2001). We determined that *Neisseria perflava*, *Lactobacillus delbrueckii* subsp. *bulgaricus*, and *Sphingobacterium faecium* are related to hormone levels. It is more common with pairs of microbes with similar functions to coexist through combinations of commensalism, complementarity, and cross-feeding of vitamins, amino acids and other co-factors (Faust *et al.*, 2012). *Neisseria perflava* has closely corresponding relationships with *Roseburia, Amaricoccus,* and *Streptomyces* species, which may execute a series of consecutive biochemical process involving TSH and T3. Thyroid carcinoma is always accompanied by a disorder of hormone secretion; excessive hormones stimulate cancer development. The roles of these specific bacteria require further study, as their intervention may promote therapeutic outcomes.

The human body is a complex ecosystem in which microbes compete and cooperate, which can support health or promote disease. Cooccurrence networks can be used to display the relationships within the microbial community. The patterns of the human microbiome are, for the most part, highly localized, along with most relationships occurring among a body site or area, and there are proportionally few strong correspondences that span even closely related body sites (Faust *et al.*, 2012). At the phylum level, compared with tumors, the cooccurrence network had more negative correlations in normal tissue. This is considered as reduced interspecies competition in tumors. Greater resource availability is thought to reduce competition in microbial communities (Hubbell, 2005; Caporaso *et al.*, 2010); thus, tumor secretions (e.g., cytokines) likely contribute to reduced competition, which may produce compounds that can be utilized for growth as well as propagation. The network of the whole thyroid gland, with more negative edges than locally interpreted, indicates that the competition increased along with the enlargement of the space scale, and the continuous marginal regions of two parts of tissue seem to be in fierce composition, indicating the shortage of necessary compounds (e.g., carbon, nitrogen) for microbial metabolism in edge areas. Network hubs or module hubs have not been observed in thyroid or gut, indicating that the structures of the network were not hub-based. The majority of the node data were categorized as connectors, with a few nodes categorized as peripheral nodes. The connector node represents a node with a high network betweenness value and can function as a bridge between modules. The microbiota community lacked a network hub, which would have had a high within-module degree as well as among-module connectivity and showed supergeneralist taxons (Poudel *et al.*, 2016). The modular structure of cooccurring OTUs suggests diversity in species character and functionality (Montoya *et al.*, 2015) as well as their environmental preferences. Thus, these microcommunities were divided into several modules (based on different preferences), and the stabilization of the network was based on several microbes that are dominant in each small module. Thus, the microenvironment of the tumor may be attributed to several dominant species (e.g., *Aggregatibacter aphrophilus* and *Pseudomonas mucidolens*) that execute different functions. From the results of functional prediction performed by Tax4Fun2, the top 30 abundant pathways from tissue and stool samples were the same that play a leading part in a series of metabolisms. However, more than half of those from the top 30 pathways were significantly different. Many diseases were accompanied by the disorder of the intestinal tract and the change of gut microbiota. Like the brain-gut axis and the gut-renal axis, the thyroid-gut-axis has been reported that gut microbiota influent the absorption of minerals relevant to the thyroid and regulate the host immune system (Knezevic *et al.*, 2020). However, the thyroid-gut-axis may not only regulate by gut microbiota, but thyroid microbes may also modify other organs by releasing secondary metabolites (active peptides, amino acids, etc.) into the circulatory system of the host, including the intestinal tract. The disorder of thyroid (thyroid carcinoma, Graves' disease, Hashimoto disease, etc.) can reflect in the alteration of gut microbiota (Ebert, 2010; Zhang *et al.*, 2019).

Undigested carbohydrates were utilized by gut microbes, forming SCFAs (including butanoate, methylacetic, and acetic acid) in healthy gut flora. Butanoate and its salt compound-butyrate, are active anti-cancer substances. It has been reported that the anti-cancer effects of butanoate include anti-inflammation and downregulation the Wnt signaling pathway. Reduction of butanoate in stool from colorectal cancer patients may not only be a biomarker of cancer risk, but also a signal of cancer progress and severity.

Butyrate is metabolized by intestinal microbes that can reverse the Warburg effect, leading to tumor apoptosis (O'Keefe, 2016; Xu *et al.*, 2017). Functional prediction and the Pearson test indicated that the combination of *Aggregatibacter aphrophilus* and *Pseudomonas mucidolens* consumed the butanoate and activated the glycolysis and gluconeogenesis in all samples, revealing the tumor microenvironment in the thyroid and gut. In addition, in Jing's study (Feng *et al.*, 2019), they detected a large quantity of compounds belonging to lipid-related metabolism in stool samples from thyroid carcinoma patients compared with the control group, which indicated a disorder in lipid metabolism. Likewise, the related pathways were present in our results. Moreover, this phenomenon is also present in thyroid tissues, and it seems that the thyroid also suffers from the excessive consumption of lipid by microbes, such as *Aggregatibacter aphrophilus*. Cysteine and methionine metabolism involved in hyperhomocysteinemia, which occurred when Homocysteine level exceed 15 μmol/L in plasma (Son and Lewis, 2021). The elevation in plasma homocysteine is considered to be related to several human cancer, along with cancer progression (Wu and Wu, 2002). Animal study found that an underlying cause of hyperhomocysteinemia in tumor-bearing rats is associated with the altered cellular methylation reactions in tumor cells and to tumor proliferation rate (Pryzimirska *et al.*, 2007). Gut as well as thyroid microbes metabolic cysteine, that may lead to high concentrate of plasma homocysteine and this result indicated a well carcinogenesis microenvironment created by

microbes.

Ecological communities often transition from phylogenetic and functional clustering to overdispersion and over succession, as judged by space-for-time substitution studies. Phylogenetically similar species (phylogenetic clustering) are often explained as the result of environmental filtering (Li *et al.*, 2015). The microbial communities in our samples lie in a primary stage of community succession. NTI had no significant correlation with increasing hormones (T3, TSH, and PTH), indicating that the phylogenetic process was more likely caused by other environmental factors.

Our study confirmed the existence of microbes in the thyroid and displayed the whole scale of microbiota in the thyroid and gut from thyroid carcinoma patients. We confirmed the existence of microbial communities in thyroid tissues. Tax4Fun2 functional prediction revealed tumor-associated microbial metabolic processes of the thyroid, and these processes may reflect the gut, leading to the disorder of gut metabolism; *Pseudomonas* mucidolens was associated with a lot of bioprocesses in the micro environment and maybe a primary pathogen in thyroid carcinoma development. The cooccurrence network showed that the margins of different thyroid tissues were unique areas, characterized by more competition, and from the topology analysis, we found that the stabilization of micro communities from tissue and stool may be maintained by several clusters of species that may execute different vital metabolism processes dominantly, attributed to the microenvironment of cancer. The nearest-taxon index indicated that the communities were standing in the primary stage of development. These results gave us new insights into the potential for therapy for thyroid carcinoma, as restraining specific microbes may promote the effectiveness of treatment and inhibit the development of cancer, but this correlation still requires further integral study.

Acknowledgements

This study was supported by the Yunnan Province Innovation Team of Intestinal Microecology Related Disease Research and Technological Transformation (China) (202005AE160010) and Yunnan Digestive Endoscopy Clinical Medical Center Foundation for Health Commission of Yunnan Province (2019LCZXKF-XH01).

Conflict of Interest

The authors have no conflict of interest to report.

Ethical Statements

The protocol for the original treatment study was approved by the Medical ethics committee of Kunming University of Science and Technology (number: KMUST-MEC-081). All research methods were performed by the relevant guidelines and regulations. For the consent process, we contacted patients or their family members and explained the study in detail.

References

Akslen, L.A., Haldorsen, T., Thoresen, S.O., and Glattre, E. 1993. Incidence pattern of thyroid cancer in Norway: influence of birth cohort and time period. *Int. J. Cancer* **53**, 183–187.

Avril, M. and Depaolo, R.W. 2021. "Driver-passenger" bacteria and their metabolites in the pathogenesis of colorectal cancer. *Gut Microbes* **13**, 1941710.

Bader, G.D. and Hogue, C.W.V. 2003. An automated method for finding molecular complexes in large protein interaction networks. *BMC Bioinformatics* **4**, 2.

Brunk, C.F. and Eis, N. 1998. Quantitative measure of small-subunit rRNA gene sequences of the kingdom *Korarchaeota*. *Appl. Environ. Microbiol.* **64**, 5064–5066.

Caporaso, J.G., Kuczynski, J., Stombaugh, J., Bittinger, K., Bushman, F.D., Costello, E.K., Fierer, N., Peña, A.G., Goodrich, J.K., Gordon, J.I., *et al.* 2010. QIIME allows analysis of high-throughput community sequencing data. *Nat. Methods* **7**, 335–336.

Chaudhary, P.P., Conway, P.L., and Schlundt, J. 2018. Methanogens in humans: potentially beneficial or harmful for health. *Appl. Microbiol. Biotechnol.* **102**, 3095–3104.

Cumbo, F., Paci, P., Santoni, D., Di Paola, L., and Giuliani, A. 2014. GIANT: a cytoscape plugin for modular networks. *PLoS ONE* **9**, e105001.

Dzieciol, M., Schornsteiner, E., Meryem-Uyar, M., Stessl, B., Wagner, M., and Schmitz-Esser, S. 2016. Bacterial diversity of floor drain biofilms and drain waters in a *Listeria monocytogenes* contaminated food processing environment. *Int. J. Food Microbiol.* **223**, 33–40.

Ebert, E.C. 2010. The thyroid and the gut. *J. Clin. Gastroenterol.* **44**, 402–406.

Faria, A.M., Gomes-Santos, A.C., Gonçalves, J.L., Moreira, T.G., Medeiros, S.R., Dourado, L.P.A., and Cara, D.C. 2013. Food components and the immune system: from tonic agents to allergens. *Front. Immunol.* **4**, 102.

Faust, K., Sathirapongsasuti, J.F., Izard, J., Segata, N., Gevers, D., Raes, J., and Huttenhower, C. 2012. Microbial co-occurrence relationships in the human microbiome. *PLoS Comput. Biol.* **8**, e1002606.

Feng, J., Zhao, F., Sun, J., Lin, B., Zhao, L., Liu, Y., Jin, Y., Li, S., Li, A., and Wei, Y. 2019. Alterations in the gut microbiota and metabolite profiles of thyroid carcinoma patients. *Int. J. Cancer* **144**, 2728–2745.

Fine, P.V.A. and Kembel, S.W. 2011. Phylogenetic community structure and phylogenetic turnover across space and edaphic gradients in western Amazonian tree communities. *Ecography* **34**, 552–565.

Gagnière, J., Bonnin, V., Jarrousse, A.S., Cardamone, E., Agus, A., Uhrhammer, N., Sauvanet, P., Dechelotte, P., Barnich, N., Bonnet, M., *et al.* 2017. Interactions between microsatellite instability and human gut colonization by *Escherichia coli* in colorectal cancer. *Clin. Sci.* **131**, 471–485.

Holmes, I., Harris, K., and Quince, C. 2012. Dirichlet multinomial mixtures: generative models for microbial metagenomics. *PLoS ONE* **7**, e30126.

Hrdina, J., Banning, A., Kipp, A., Loh, G., Blaut, M., and Brigelius-Flohé, R. 2009. The gastrointestinal microbiota affects the selenium status and selenoprotein expression in mice. *J. Nutr. Biochem.* **20**, 638–648.

Hu, X., Wang, T., and Jin, F. 2016. Alzheimer's disease and gut microbiota. *Sci. China Life Sci.* **59**, 1006–1023.

Hubbell, S.P. 2005. Neutral theory in community ecology and the hypothesis of functional equivalence. *Funct. Ecol.* **19**, 166–172.

Jackson, M.A., Verdi, S., Maxan, M.E., Shin, C.M., Zierer, J., Bowyer, R.C.E., Martin, T., Williams, F.M.K., Menni, C., Bell, J.T., *et al.* 2018. Gut microbiota associations with common diseases and prescription medications in a population-based cohort. *Nat. Com-*

mun. **9**, 2655.
Jia, B. 2019. Commentary: gut microbiome–mediated bile acid metabolism regulates liver cancer via NKT cells. *Front. Immunol.* **10**, 282.
Kembel, S.W., Cowan, P.D., Helmus, M.R., Cornwell, W.K., Morlon, H., Ackerly, D.D., Blomberg, S.P., and Webb, C.O. 2010. Picante: R tools for integrating phylogenies and ecology. *Bioinformatics* **26**, 1463–1464.
Knezevic, J., Starchl, C., Tmava Berisha, A., and Amrein, K. 2020. Thyroid-gut-axis: how does the microbiota influence thyroid function? *Nutrients* **12**, 1769.
Kumar, S., Stecher, G., Li, M., Knyaz, C., and Tamura, K. 2018. MEGA X: molecular evolutionary genetics analysis across computing platforms. *Mol. Biol. Evol.* **35**, 1547–1549.
Lauritano, E.C., Bilotta, A.L., Gabrielli, M., Scarpellini, E., Lupascu, A., Laginestra, A., Novi, M., Sottili, S., Serricchio, M., Cammarota, G., *et al.* 2007. Association between hypothyroidism and small intestinal bacterial overgrowth. *J. Clin. Endocrinol. Metab.* **92**, 4180–4184.
Leshem, Y. and Pastan, I. 2019. *Pseudomonas* exotoxin immunotoxins and anti-tumor immunity: from observations at the patient's bedside to evaluation in preclinical models. *Toxins* **11**, 20.
Li, S., Cadotte, M., Meiners, S., Hua, Z., Jiang, L., and Shu, W. 2015. Species colonisation, not competitive exclusion, drives community overdispersion over long-term succession. *Ecol. Lett.* **18**, 964–973.
Liu, S., Semenciw, R., Ugnat, A.M., and Mao, Y. 2001. Increasing thyroid cancer incidence in Canada, 1970-1996: time trends and age-period-cohort effects. *Br. J. Cancer* **85**, 1335–1339.
Londero, S.C., Krogdahl, A., Bastholt, L., Overgaard, J., Pedersen, H.B., Hahn, C.H., Bentzen, J., Schytte, S., Christiansen, P., Gerke, O., *et al.* 2015. Papillary thyroid carcinoma in Denmark, 1996–2008: outcome and evaluation of established prognostic scoring systems in a prospective national cohort. *Thyroid* **25**, 78–84.
Lubina, A., Cohen, O., Barchana, M., Liphshiz, I., Vered, I., Sadetzki, S., and Karasik, A. 2006. Time trends of incidence rates of thyroid cancer in Israel: what might explain the sharp increase. *Thyroid* **16**, 1033–1040.
Markou, P. and Apidianakis, Y. 2014. Pathogenesis of intestinal *Pseudomonas aeruginosa* infection in patients with cancer. *Front. Cell. Infect. Microbiol.* **3**, 115.
McNally, R.J.Q., Blakey, K., James, P.W., Pozo, B.G., Basta, N.O., and Hale, J. 2010. Increasing incidence of thyroid cancer in Great Britain, 1976-2005: age-period-cohort analysis. *J. Epidemiol. Community Health* **64**, A31. https://jech.bmj.com/content/64/Suppl_1/A31.2.
Montoya, D., Yallop, M.L., and Memmott, J. 2015. Functional group diversity increases with modularity in complex food webs. *Nat. Commun.* **6**, 7379.
Nejman, D., Livyatan, I., Fuks, G., Gavert, N., Zwang, Y., Geller, L.T., Rotter-Maskowitz, A., Weiser, R., Mallel, G., Gigi, E., *et al.* 2020. The human tumor microbiome is composed of tumor type–specific intracellular bacteria. *Science* **368**, 973–980.
NIH/National Cancer Institute. 2018. Gut microbiome can control antitumor immune function in liver. Science Daily. www.sciencedaily.com/releases/2018/05/180524141715.htm.
Nikiforov, Y.E. 2008. Thyroid carcinoma: molecular pathways and therapeutic targets. *Mod. Pathol.* **21**, S37–S43.
Nussey, S. and Whitehead, S. 2001. Endocrinology: An Integrated Approach. Oxford: BIOS Scientific Publishers, Milton Park, England. https://www.ncbi.nlm.nih.gov/books/NBK22/.
O'Keefe, S.J.D. 2016. Diet, microorganisms and their metabolites, and colon cancer. *Nat. Rev. Gastroenterol. Hepatol.* **13**, 691–706.
Olaleye, O., Ekrikpo, U., Moorthy, R., Lyne, O., Wiseberg, J., Black, M., and Mitchell, D. 2011. Increasing incidence of differentiated thyroid cancer in South East England: 1987-2006. *Eur. Arch. Otorhinolaryngol.* **268**, 899–906.
Parkins, M.D., Somayaji, R., and Waters, V.J. 2018. Epidemiology, biology, and impact of clonal *Pseudomonas aeruginosa* infections in cystic fibrosis. *Clin. Microbiol. Rev.* **31**, e00019-18.
Poudel, R., Jumpponen, A., Schlatter, D.C., Paulitz, T.C., McSpadden Gardener, B.B., Kinkel, L.L., and Garrett, K.A. 2016. Microbiome networks: a systems framework for identifying candidate microbial assemblages for disease management. *Phytopathology* **106**, 1083–1096.
Pruesse, E., Quast, C., Knittel, K., Fuchs, B.M., Ludwig, W., Peplies, J., and Glöckner, F.O. 2007. SILVA: a comprehensive online resource for quality checked and aligned ribosomal RNA sequence data compatible with ARB. *Nucleic Acids Res.* **35**, 7188–7196.
Pryzimirska, T.V., Pogribny, I.P., and Chekhun, V.F. 2007. The impact of tumor growth on plasma homocysteine levels and tissue-specific DNA methylation in Walker-256 tumor-bearing rats. *Exp. Oncol.* **29**, 262–266.
Rahib, L., Smith, B.D., Aizenberg, R., Rosenzweig, A.B., Fleshman, J.M., and Matrisian, L.M. 2014. Projecting cancer incidence and deaths to 2030: the unexpected burden of thyroid, liver, and pancreas cancers in the United States. *Cancer Res* **74**, 2913–2921.
Reysenbach, A.L., Giver, L.J., Wickham, G.S., and Pace, N.R. 1992. Differential amplification of rRNA genes by polymerase chain reaction. *Appl. Environ. Microbiol.* **58**, 3417–3418.
Saika, K., Matsuda, T., and Sobue, T. 2014. Incidence rate of thyroid cancer by histological type in Japan. *Jpn. J. Clin. Oncol.* **44**, 1131–1132.
Scales, B.S., Dickson, R.P., LiPuma, J.J., and Huffnagle, G.B. 2014. Microbiology, genomics, and clinical significance of the *Pseudomonas fluorescens* species complex, an unappreciated colonizer of humans. *Clin. Microbiol. Rev.* **27**, 927–948.
Schloss, P.D., Westcott, S.L., Ryabin, T., Hall, J.R., Hartmann, M., Hollister, E.B., Lesniewski, R.A., Oakley, B.B., Parks, D.H., Robinson, C.J., *et al.* 2009. Introducing mothur: open-source, platform-independent, community-supported software for describing and comparing microbial communities. *Appl. Environ. Microbiol.* **75**, 7537–7541.
Schmidt, T.M., DeLong, E.F., and Pace, N.R. 1991. Analysis of a marine picoplankton community by 16S rRNA gene cloning and sequencing. *J. Bacteriol.* **173**, 4371–4378.
Shin, N.R., Whon, T.W., and Bae, J.W. 2015. Proteobacteria: microbial signature of dysbiosis in gut microbiota. *Trends Biotechnol.* **33**, 496–503.
Son, P. and Lewis, L. 2021. Hyperhomocysteinemia. StatPearls Publishing. https://www.ncbi.nlm.nih.gov/books/NBK554408/.
Stegen, J.C., Lin, X., Fredrickson, J.K., Chen, X., Kennedy, D.W., Murray, C.J., Rockhold, M.L., and Konopka, A. 2013. Quantifying community assembly processes and identifying features that impose them. *ISME J.* **7**, 2069–2079.
Stegen, J.C., Lin, X., Konopka, A.E., and Fredrickson, J.K. 2012. Stochastic and deterministic assembly processes in subsurface microbial communities. *ISME J.* **6**, 1653–1664.
Tahmourespour, A., Ahmadi, A., and Fesharaki, M. 2020. The anti-tumor activity of exopolysaccharides from *Pseudomonas* strains against HT-29 colorectal cancer cell line. *Int. J. Biol. Macromol.* **149**, 1072–1076.
Tlaskalová-Hogenová, H., Štěpánková, R., Kozáková, H., Hudcovic, T., Vannucci, L., Tučková, L., Rossmann, P., Hrnčíř, T., Kverka, M., Zákostelská, Z., *et al.* 2011. The role of gut microbiota (commensal bacteria) and the mucosal barrier in the pathogenesis of inflammatory and autoimmune diseases and cancer: contribution of germ-free and gnotobiotic animal models of human diseases. *Cell. Mol. Immunol.* **8**, 110–120.
Ueno, K. and Shetty, K. 1997. Effect of selected polysaccharide-producing soil bacteria on hyperhydricity control in oregano tissue cultures. *Appl. Environ. Microbiol.* **63**, 767–770.
Virili, C., and Centanni, M. 2015. Does microbiota composition affect thyroid homeostasis? *Endocrine* **49**, 583–587.

Vuong, H.E. and Hsiao, E.Y. 2017. Emerging roles for the gut microbiome in autism spectrum disorder. *Biol. Psychiatry* **81**, 411–423.

Wang, J., Shen, J., Wu, Y., Tu, C., Soininen, J., Stegen, J.C., He, J., Liu, X., Zhang, L., and Zhang, E. 2013. Phylogenetic beta diversity in bacterial assemblages across ecosystems: deterministic versus stochastic processes. *ISME J.* **7**, 1310–1321.

Wang, Y. and Wang, W. 2015. Increasing incidence of thyroid cancer in Shanghai, China, 1983–2007. *Asia Pac. J. Public Health* **27**, NP223–NP229.

Wemheuer, F., Taylor, J.A., Daniel, R., Johnston, E., Meinicke, P., Thomas, T., and Wemheuer, B. 2020. Tax4Fun2: a R-based tool for the rapid prediction of habitat-specific functional profiles and functional redundancy based on 16S rRNA gene marker gene sequences. *Environ. Microbiome* **15**, 11.

Wu, D.C., Chan, W.W., Metelitsa, A.I., Fiorillo, L., and Lin, A.N. 2011. *Pseudomonas* skin infection: clinical features, epidemiology, and management. *Am. J. Clin. Dermatol.* **12**, 157–169.

Wu, L.L. and Wu, J.T. 2002. Hyperhomocysteinemia is a risk factor for cancer and a new potential tumor marker. *Clin. Chim. Acta* **322**, 21–28.

Wypych, T.P., Wickramasinghe, L.C., and Marsland, B.J. 2019. The influence of the microbiome on respiratory health. *Nat. Immunol.* **20**, 1279–1290.

Xie, S.H., Chen, J., Zhang, B., Wang, F., Li, S.S., Xie, C.H., Tse, L.A., and Cheng, J.Q. 2014. Time trends and age-period-cohort analyses on incidence rates of thyroid cancer in Shanghai and Hong Kong. *BMC Cancer* **14**, 975.

Xu, S., Liu, C.X., Xu, W., Huang, L., Zhao, J.Y., and Zhao, S.M. 2017. Butyrate induces apoptosis by activating PDC and inhibiting complex I through SIRT3 inactivation. *Sig. Transduct. Target. Ther.* **2**, 16035.

Yu, T., Guo, F., Yu, Y., Sun, T., Ma, D., Han, J., Qian, Y., Kryczek, I., Sun, D., Nagarsheth, N., *et al.* 2017. *Fusobacterium nucleatum* promotes chemoresistance to colorectal cancer by modulating autophagy. *Cell* **170**, 548–563.e16.

Zhang, J., Zhang, F., Zhao, C., Xu, Q., Liang, C., Yang, Y., Wang, H., Shang, Y., Wang, Y., Mu, X., *et al.* 2019. Dysbiosis of the gut microbiome is associated with thyroid cancer and thyroid nodules and correlated with clinical index of thyroid function. *Endocrine* **64**, 564–574.

Zheng, T., Holford, T.R., Chen, Y., Ma, J.Z., Flannery, J., Liu, W., Russi, M., and Boyle, P. 1996. Time trend and age-period-cohort effect on incidence of thyroid cancer in Connecticut, 1935-1992. *Int. J. Cancer* **67**, 504–509.

Zhou, L., Li, X., Ahmed, A., Wu, D., Liu, L., Qiu, J., Yan, Y., Jin, M., and Xin, Y. 2014. Gut microbe analysis between hyperthyroid and healthy individuals. *Curr. Microbiol.* **69**, 675–680.